JOURNAL OF MATERIALS SCIENCE 31 (1996) 4975–4980

Preparation of ZrO_2–Al_2O_3 powder by thermal decomposition of gels produced from an aluminium chelate compound and zirconium butoxide

HIDEYUKI YOSHIMATSU*, KOJI KAWABATA*, AKIYOSHI OSAKA‡, YOSHINARI MIURA§, HITOSHI KAWASAKI*
*Industrial Technology Center of Okayama Prefecture, 5301, Haga, Okayama-shi, 701-12, Japan and
‡Department of Bioscience and Technology
§Department of Environmental Chemistry and Materials, Faculty of Environmental Science and Technology, Okayama University, 2-1-1, Tsushima Naka, Okayama-shi, 700, Japan

Organic precursors containing Al and Zr atoms were synthesized from an aluminium chelate compound and zirconium n-butoxide. A ZrO_2–Al_2O_3 composite powder was prepared by the thermal decomposition of these precursors. An amorphous phase exists to higher temperatures for this ZrO_2–Al_2O_3 powder than for a comparable powder prepared from aluminium sec-butoxide and zirconium n-butoxide. In addition the tetragonal ZrO_2 phase was stabler in this ZrO_2–Al_2O_3 powder than in a comparison powder. The ZrO_2 grains were 50–500 nm in diameter and were homogeneously dispersed in the Al_2O_3 matrix after heating at 1400 °C.

1. Introduction

High performance and new functions are promised for nanocomposite materials in which nano meter sized components are homogeneously dispersed in matrix components [1–4]. ZrO_2–Al_2O_3 composite materials have been prepared by means of the hydrolysis of alkoxides [2], the co-precipitation in aqueous solutions of inorganic compounds [5], and by chemical vapour deposition [3]. We have prepared tetragonal ZrO_2 (t-ZrO_2) dispersed in an Al_2O_3 matrix powder by the thermal decomposition of Zr–Al metallo–organic compounds (zircoaluminates) [6–9]. The key feature of this method consists of the use of the metallo–organic precursors to produce the composite powder containing particles in which fine t-ZrO_2 grains are homogeneously dispersed. Unfortunately, the zircoaluminates have the following disadvantages. (1) It is hard to control the Zr to Al ratio because the zircoaluminates are commercial reagents with fixed Zr to Al ratios. (2) Their structures are unknown and (3) they contain a small concentration of impurities.

In this paper, we report the synthesis, with high purity, of organic precursor gels from an aluminium chelate compound and zirconium n-butoxide (denoted as ZNBD). We have thermally decomposed the dried gels and obtained an ZrO_2–Al_2O_3 composite powder. The properties and a suggested structure for the dried gels and heated powder are compared with those of the powders prepared by the hydrolysis of aluminium sec-butoxide (denoted as ASBD) and ZNBD and also the powder prepared from the zircoaluminates.

2. Experimental procedure

Ethyl acetoacetate aluminium di-isopropylate (denoted as ALCH) [10] is a chelate compound of aluminium and a viscous liquid. Fig. 1 illustrates the monomeric structure of this material. Mixtures of ALCH and ZNBD (0.3 mol in total) were dissolved in ethyl alcohol (3 mol) in such a manner so as to vary the ZrO_2 content from 0–100 %. The solutions were gelled at 30 °C by the addition at a rate of 0.5 ml sec^{-1} of a 9:3 molar ratio mixture of distilled water and ethyl alcohol. The precursor gels were kept at 50 °C for 12 h in air, dried at 50 °C for 6 h in vacuum, and ground. The dry gels were heated at a rate of 300 °C h^{-1} up to 700–1400 °C in air, held at those temperatures for 2 h, and cooled down in the furnace by turning off the power. Another composite powder was prepared for comparison purposes by using ASBD instead of ALCH. The procedure was similar to that used for the ALCH-derived precursor, with isopropyl alcohol replacing the ethyl alcohol as the solvent and in the gelling solution. The samples prepared from ALCH and ZNBD are denoted as the AZ system, whilst those from ASBD and ZNBD are denoted as the ALK system.

DTA curves were taken and the weight loss after heating at 1000 °C was recorded and also the carbon content was measured for the AZ dry gels. This information will be used later in the paper to help elucidate the structure of the synthesized precursors. The crystalline phases in the heated powders of the AZ and ALK systems were identified using the X-ray

0022–2461

diffraction (XRD) technique with CuK_α radiation. Hence in addition the precipitation temperature of the t-ZrO_2 phase was determined. The volume percentage (V_t) of the t-ZrO_2 phase in the total ZrO_2 concentration was evaluated by Equation 1 [11] where X_m represents the ratio of the X-ray intensities I(hkl) defined by Equation 2. The suffixes m and t indicate the monoclinic ZrO_2 (m-ZrO_2) and t-ZrO_2 phases, respectively. V_t represents the stability of the t-ZrO_2 phase in the composite powder which is important since the t-ZrO_2 modification is the unstable ZrO_2 phase at room temperature.

$$V_t = \frac{1 - X_m}{1 + 0.311X_m} \times 100(\%) \quad (1)$$

$$X_m = \frac{I_m(\bar{1}11) + I_m(111)}{I_t(101) + I_m(\bar{1}11) + I_m(111)} \quad (2)$$

Brunauer–Emmett–Teller (BET) specific surface area (SSA), of the heated powder was determined by a dynamic flow method. The average (median) particle diameter of the heated powder was measured with a particle distribution analyser by a laser diffraction method. The morphology of the heated powder was observed under a scanning electron microscope (SEM).

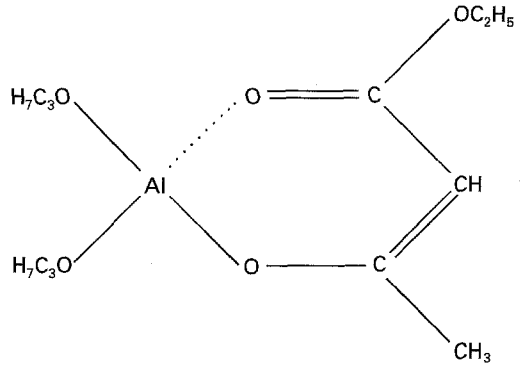

Figure 1 The structure of ethyl acetoaetate aluminium di-isopropylate (ALCH).

3. Results

3.1 Appearance and DTA curves for the gels

Table I summarizes the composition and appearance of the precursor gels of the AZ and ALK systems. The gels of AZO to AZ4 were transparent and gelatinous, whilst the gels AZ6 and AZ7 and ALKO to ALK6 were opaque precipitations. The AZ5 gel showed an opaque gelatinous appearance which may be due to a mixture of gelation and precipitation. These results indicated that the ZNBD which is present in the precursor gels AZ1 to AZ4 was not precipitated with water. Fig. 2 illustrates the DTA curves for the dry gels of AZ0, AZ2, AZ4 and AZ7. Sharp and broad exothermic peaks around 230 °C and 400 °C due to the oxidation of organic components were observed for the AZ0 dry gel. Similar curves were obtained for the dry gels of AZ2 and AZ4. A different pattern was observed for the AZ7 dry gel consisting of broad peaks around 200 °C and 300 °C, a shoulder peak around 260 °C, and a sharp peak around 430 °C. Thus, the appearance and thermal decomposition behaviour of the gels of AZ system depended on the Al:Zr molar ratios. The gels of AZ1 to AZ4 with a molar ratio $\geqslant$2:1 were similar to AZ0 with respect to these features.

3.2 Crystalline phase present, and SEM photographs of, the heated powder

Table II summarizes the crystalline phases in the AZ powder after the heat treatment up to 1400 °C. The AZ0 powder, consisting only of Al_2O_3, mainly gave broad XRD peaks of the tetragonal Al_2O_3 phase in the range from 800 °C to 1000 °C and sharp peaks of the Al_2O_3 rhombohedral phase for temperatures >1100 °C. The AZ7 powder, consisting only of ZrO_2, mainly gave sharp peaks of the monoclinic phase in the range from 700–1400 °C. The powders of AZ1–AZ6 were amorphous at lower temperatures, and broad t-ZrO_2 peaks were detected after the heat treatments between 800–1000 °C, whereas t-ZrO_2, m-ZrO_2 and rhombohedral Al_2O_3 were the main

TABLE I Composition and appearance of the precursor gels of AZ and ALK systems

Sample	Molar ratio Al:Zr	ZrO_2 content (vol %)*	Appearance
AZ0	only Al	0	
AZ1	8:1	16.5	
AZ2	4:1	28.3	transparent, gelatinous
AZ3	3:1	34.5	
AZ4	2:1	44.1	
AZ5	1:1	61.3	opaque, gelatinous
AZ6	1:2	76.0	opaque, precipitation
AZ7	only Zr	100	
ALK0	only Al	0	
ALK1	8:1	16.5	
ALK2	4:1	28.3	
ALK3	3:1	34.5	opaque, precipitation
ALK4	2:1	44.1	
ALK5	1:1	61.3	
ALK6	1:2	76.0	

*In the heated powder.

phases after the $>1200\,^{\circ}C$ heat treatments. The crystalline phases found in the ALK powder were similar to those for the AZ powder.

Fig. 3 shows SEM photographs for the AZ2 and ALK2 powder after heating at 800 °C and 1400 °C. The AZ2 powder had a homogeneous surface after heating at 800 °C because ZrO_2 was not squeezed out of the Al_2O_3 matrix. Fine grains 100–300 nm in diameter were dispersed in the AZ2 particle after heating at 1400 °C. We previously reported that the grains and matrix consist of ZrO_2 and Al_2O_3, respectively [9]. On the other hand, aggregates of primary particles for the ALK2 powder shown in Fig. 3c were sintered at 1400 °C to form secondary particles as indicated in Fig. 3d. Since the ZrO_2 grains in the ALK2 particle could not be observed under the SEM, the grain size could not be estimated. Fig. 4 shows the SEM photographs for the powder of AZ1, AZ2, AZ4 and AZ5 after heating at 1400 °C. The diameter of the ZrO_2 grains increased from about 50 nm to 500 nm with increasing ZrO_2 content, and these grains were homogeneously dispersed in the particle for all the powders.

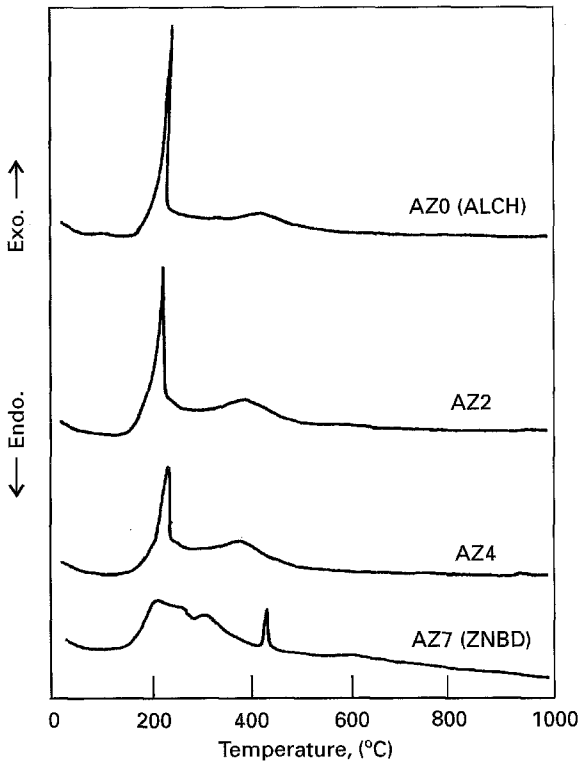

Figure 2 DTA curves for the dry gels prepared from ALCH and ZNBD.

3.3 Precipitation temperature of t-ZrO_2 and V_t

Fig. 5 shows the precipitation temperature of the t-ZrO_2 phase as a function of ZrO_2 content for the AZ and ALK powders. The precipitation temperature was 1000 °C for the powders of AZ1 to AZ3, and decreased with increasing the ZrO_2 content until it reached 800 °C for the AZ6 powder. The AZ powders had a higher precipitation temperature than the ALK powders except for the AZ4 powder. The results indicated that the AZ powder remained amorphous up to a higher temperature than the ALK powder.

Fig. 6 illustrates the fraction V_t of t-ZrO_2 as a function of ZrO_2 content for the AZ and ALK powders after heating at 1400 °C. This V_t value of the AZ powder decreased with increasing the ZrO_2 content, but remained $>90\,\%$ in the range <30 vol % ZrO_2 content. The AZ powder had higher V_t than than the ALK powder in the range <40 vol % ZrO_2 content though they had similar V_t values in the range >40 vol %. In particular, the difference in V_t between the AZ and ALK powders was large in the range between 28–35 vol %. Since V_t for the zircoaluminate-derived powder with 16 and 20 vol % ZrO_2 content was 100 and 94 %, respectively [6, 7], t-ZrO_2 in the AZ powder is equally stable as it is in the zircoaluminate-derived powder.

3.4 Specific surface area (SSA)

The average (median) particle diameter of the AZ2 and ALK2 powder was 10 and 15 μm, respectively. Fig. 7 illustrates the specific surface area (SSA) for the AZ2 and ALK2 powder as a function of the heating

TABLE II Crystalline phase in the heated powders of the AZ system

Temp. (°C)	AZ0	AZ2	AZ4	AZ6	AZ7
1400			TZ, MZ, RA		MZ
1300	RA				
1200		TZ, RA, TA, MA		TZ, MZ, TA, MA	
1100	RA, TA, MA	TZ, TA			
1000				TZ	TZ
900	TA				MZ
800		amorphous			
700					

TZ: tetragonal ZrO_2 (JCPDS 241164)
MZ: monoclinic ZrO_2 (JCPDS 360420)
RA: rhombohedral Al_2O_3 (α-Al_2O_3) (JCPDS 100173)
TA: tetragonal Al_2O_3 (JCPDS 160394)
MA: monoclinic Al_2O_3 (JCPDS 350121)

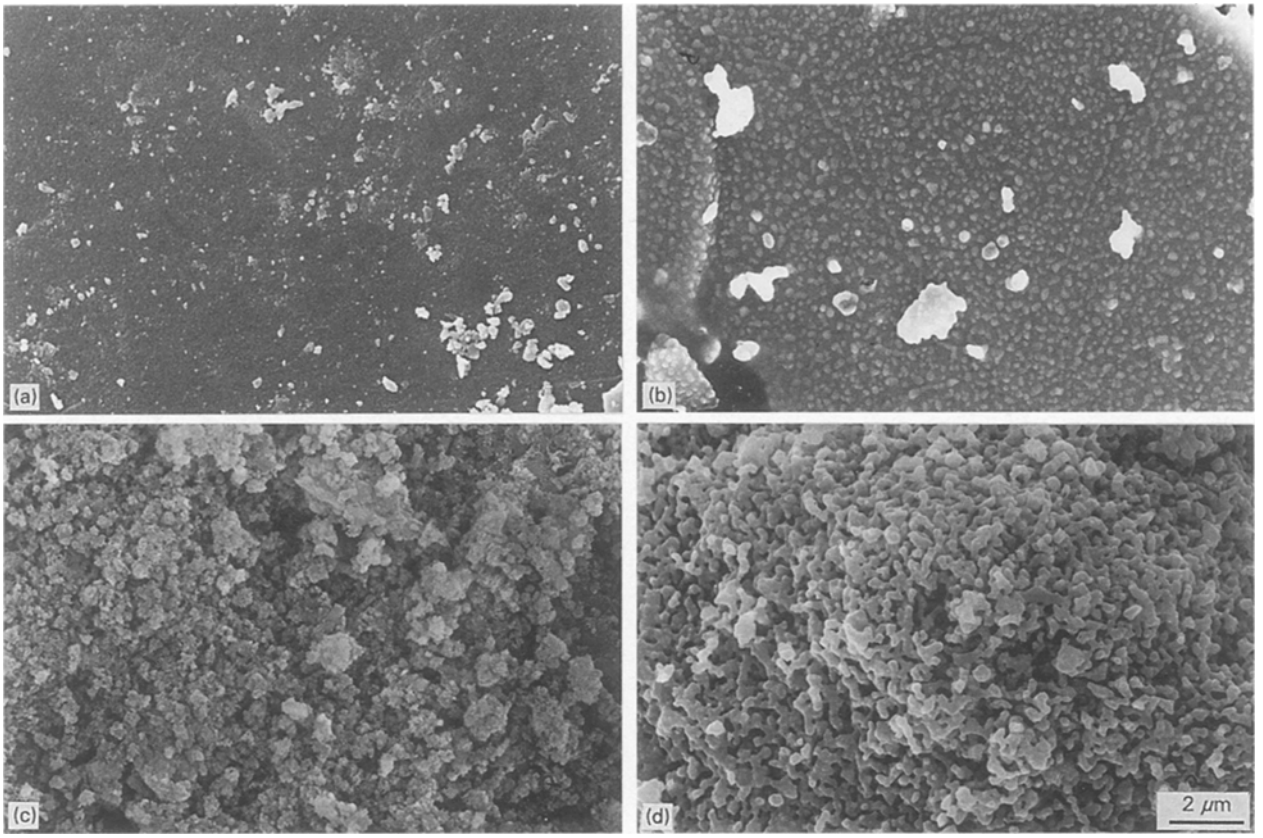

Figure 3 Scanning electron micrographs of AZ and ALK powders. (a) AZ2 powder after heating at 800 °C for 2 h, (b) AZ2 powder after heating at 1400 °C for 2 h, (c) ALK2 powder after heating at 800 °C for 2 h, (d) ALK2 powder after heating at 1400 °C for 2 h.

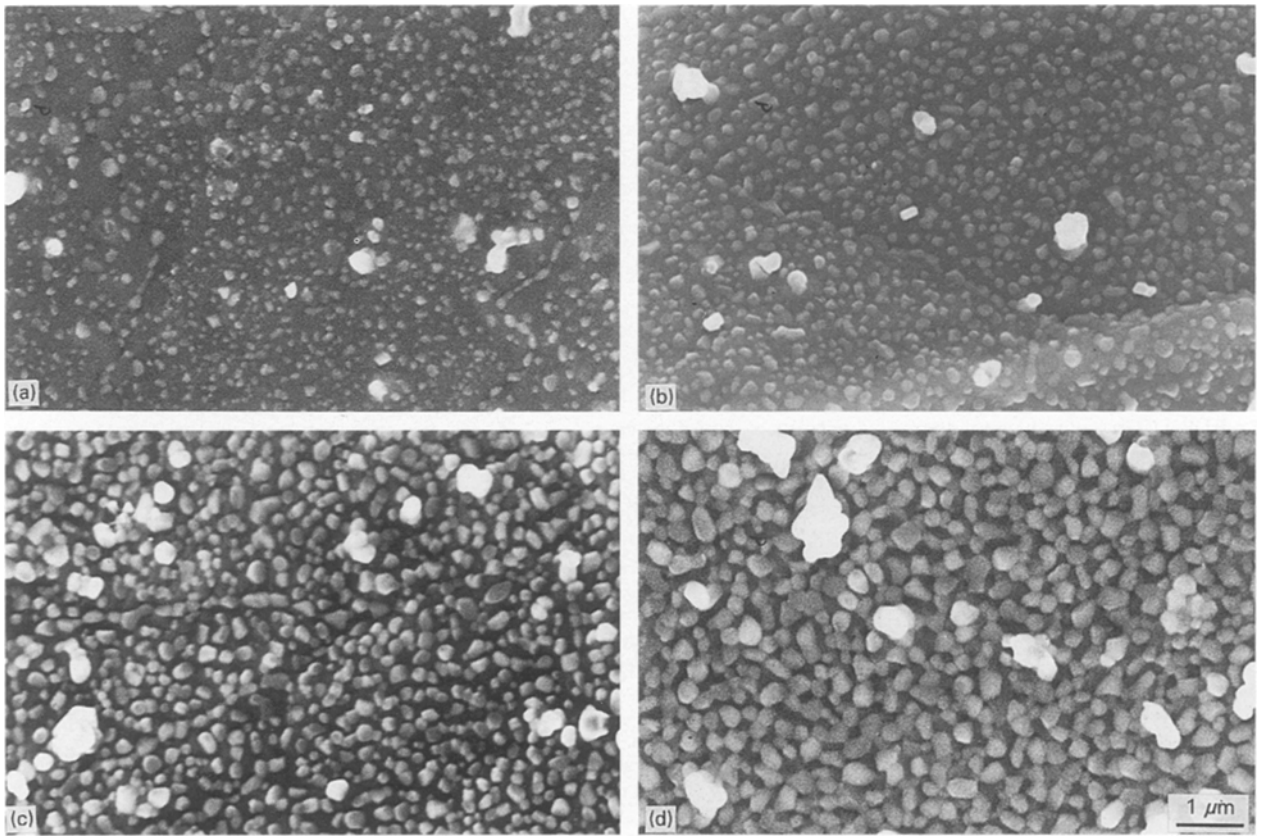

Figure 4 Scanning electron micrographs of the powder of (a) AZ1, (b) AZ2, (c) AZ4 and (d) AZ5 after heating at 1400 °C for 2 h.

temperature. The SSA for the AZ2 powder heated between 700–900 °C was greater than 200 $m^2 g^{-1}$, whilst the ALK2 powder could never exceed 200 $m^2 g^{-1}$ in SSA. After heating at a temperature $\geq$ 1100 °C, the SSA of the AZ2 powder was less than 1 $m^2 g^{-1}$, whilst that of the ALK2 was more than 10 $m^2 g^{-1}$. Thus, the SSA for the AZ2 powder was heavily dependent on the heating temperature.

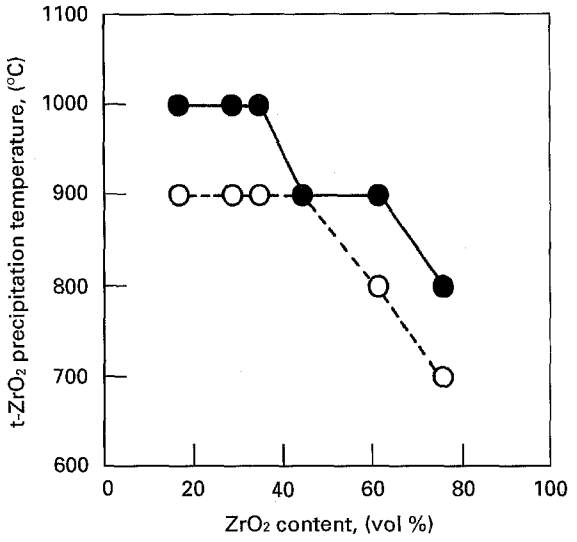

Figure 5 The precipitation temperature of tetragonal ZrO_2 for the (●) AZ powder and (○) ALK powder as a function of ZrO_2 content.

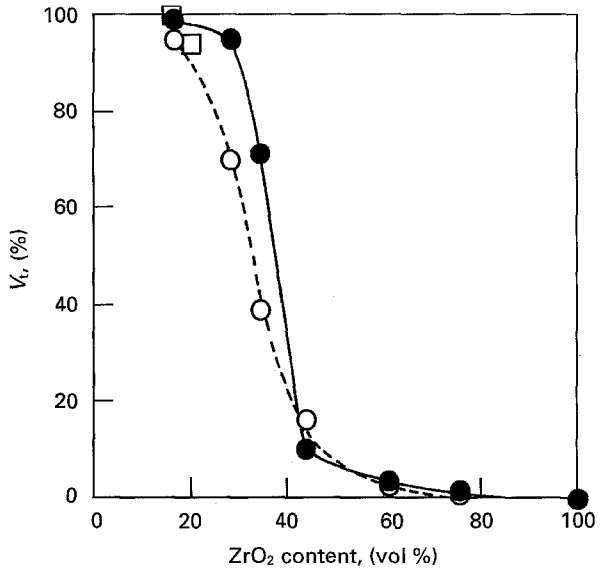

Figure 6 The fraction V_t of tetragonal ZrO_2 for the (●) AZ powder, (○) ALK powder and (□) zircoaluminate-derived powder [6, 7] after heating at 1400 °C for 2 h as a function of ZrO_2 content.

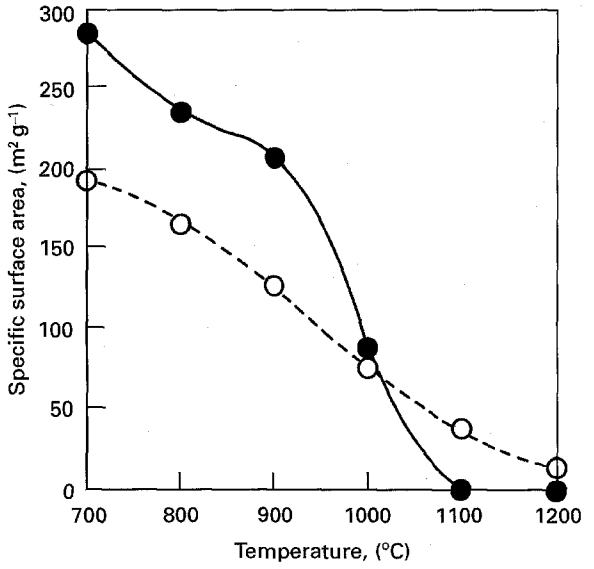

Figure 7 The specific surface area for the (●) AZ2 powder and (○) ALK2 powder as a function of the heating temperature.

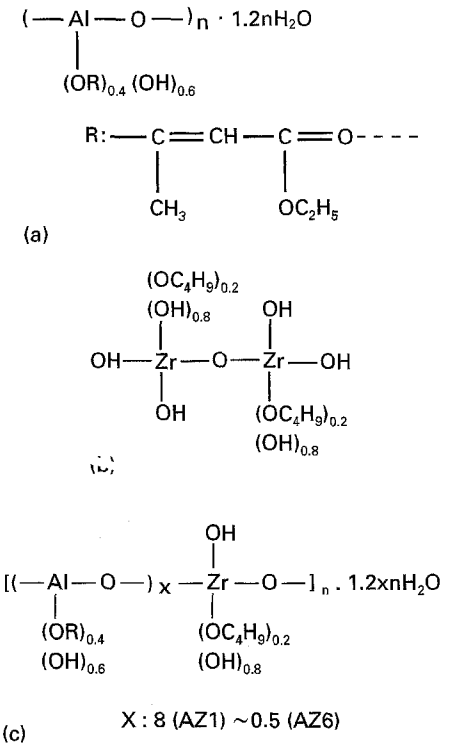

Figure 8 Models of the structures for the dry gels prepared from (a) ALCH, (b) ZNBD and (c) ALCH and ZNBD (ALCH-ZNBD gels).

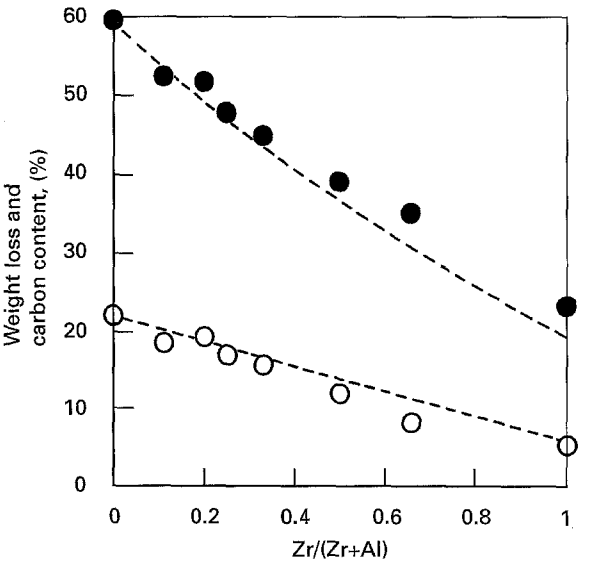

Figure 9 (●) Weight loss for the dry gel after heating at 1000 °C for 2 h and (○) carbon content in the dry gels as a function of Zr/(Zr + Al) molar ratio. points: based on the measured data, dashed line: calculated data based on Fig. 8(c).

4. Discussion

4.1 Structure of gels from ALCH and ZNBD

The appearance and thermal decomposition behaviour of the gels for the molar ratios Al:Zr of 8:1 to 2:1 (AZ1 to AZ4) are similar to those of the AZ0 gel (ALCH gel) as is shown in Table I and Fig. 2. The results suggest the formation of similar complexes between ALCH and ZNBD at mixing or gelation. Such complex gels of ALCH and ZNBD are hereafter denoted as ALCH–ZNBD gels. Since ALCH is polymerized in the form of $(-Al(OH)-O-)_n$ or $(-Al(OR)$

$-O-)_n$ ($R = -C(CH_3)=CH-C(OC_2H_5)=O-$) in the presence of H_2O [12], the ALCH gel can be presented as $(-Al[OR)_x(OH)_{1-x}]-O-)_n$. The fraction x of the OR groups bonded to Al has been evaluated with the weight loss (= 59.7 %) and carbon content (= 22.1 %). Thus the structure of the AZ0 dry gel can be represented as illustrated in Fig. 8a. In a similar way, the structure of the AZ7 dry gel (ZNBD gel) is derived on the basis of the weight loss (= 23.3 %) and carbon content (= 5.5 %) and is illustrated in Fig. 8b. If ZNBD and ALCH form complex ALCH–ZNBD gels, a structural model can be proposed as illustrated in Fig. 8c where Zr is incorporated in the –Al–O– chains. Fig. 9 illustrates the measured weight loss and carbon content for the dry gels in addition to those calculated on the basis of the model in Fig. 8c as a function of the Zr/(Zr + Al) molar ratio. The calculated weight loss and carbon content agree well with the measured ones for the dry gels of AZ1 through AZ4 (Zr/(Zr + Al) < 0.35). These gels were similar in appearance (transparent gelation) to the AZ0 gel. However, the calculated values for the AZ5 and AZ6 dry gels (Zr/(Zr + Al) > 0.35) deviated from the measured ones, and the appearance of the gels were different from that of AZ0 gel. The results suggest that the model in Fig. 8c closely represents the structures of the dry gels of AZ1 to AZ4 but is not applicable to the AZ5 and AZ6 dry gels.

4.2 Dispersion of ZrO_2 and Al_2O_3

The homogeneity of the dispersion of ZrO_2 and Al_2O_3 for the AZ powder is discussed here on the basis of Figs 3–6. The ZrO_2 component in the ZrO_2–Al_2O_3 powder precipitates into grains with increasing heating temperature [9]. Fig. 5 has indicated that the t-ZrO_2 phase is harder to precipitate for the AZ powder than for the ALK one. Zr and Al atoms in the AZ precursor are mixed on an atomic scale as suggested in Fig. 8c. Under these circumstances it is difficult for the Zr atoms to cluster together in order to begin forming a crystal lattice, and the t-ZrO_2 phase is precipitated consequently at a higher temperature for the AZ powder. On the other hand, ALK powder consists of aggregates of amorphous ZrO_2 primary particles and amorphous Al_2O_3 ones as indicated in Fig. 3c. Thus, the ZrO_2 primary particles are easily crystallized, and the t-ZrO_2 phase consequently precipitates at a lower temperature. The AZ powder therefore can be applied as a catalyser taking advantage of the high homogeneity of dispersion of ZrO_2 and Al_2O_3 as well as the large SSA shown Fig. 7.

The t-ZrO_2 grain size grows with increasing heating temperature for the ZrO_2–Al_2O_3 powder. Since the dispersed ZrO_2 grains are fine, t-ZrO_2 can be quenched to room temperature. However, when the ZrO_2 grain size exceeds a threshold (critical size), the tetragonal phase transforms to the monoclinic phase during the cooling to room temperature [5]. Thus the smaller grain size is directly related with the larger values in V_t. Since V_t for the AZ powder is higher than that for the ALK one in the range of ZrO_2 content < 40 vol %, it is suggested that the ZrO_2 grains dispersed in the AZ powder are finer than those dispersed in the ALK one. The decrease in V_t with the ZrO_2 content, illustrated in Fig. 6, is therefore attributed to the ZrO_2 grain growth which has been observed in Fig. 4. V_t and the grain size can be estimated from Figs 4 and 6 to be 95 % and 100–300 nm in diameter for the AZ2 powder, and 4 % and 200–500 nm for the AZ5 one. Therefore, the critical size for the transformation is calculated to be 200–300 nm for the AZ powder, though 600 nm has been assigned to the critical size by Heuer *et al.* for ZrO_2 dispersed in Al_2O_3 dense ceramics [5]. One of the possible reasons for the difference in the critical size is the difference in the form of the Al_2O_3 matrix, in our case powder as against a sintered bulk.

5. Conclusions

The aluminium chelate compound (ALCH) and zirconium n-butoxide were gelled to form the organic precursors composed of Al and Zr atoms. The precursors were thermally decomposed to prepare the ZrO_2–Al_2O_3 composite powder (AZ powder). The diameter of the ZrO_2 grains increased from about 50 to 500 nm with increasing ZrO_2 content, and these grains were homogeneously dispersed in the Al_2O_3 matrix for the AZ powder after heating at 1400 °C. The precipitation temperature of t-ZrO_2 and t-ZrO_2 content (V_t) are higher for the AZ powder than for the ALK powder prepared from aluminium sec-butoxide and zirconium n-butoxide. The specific surface area for the AZ powder was drastically dependent on the heating temperature. It is concluded that ZrO_2 and Al_2O_3 were homogeneously composed in the nano meter scale for the AZ powder.

References

1. A. NAKAHARA and K. NIIHARA, *Seramikkusu* (*Bull. Ceram. Soc. Jpn*) **26** (1991) 218.
2. P. F. BECHER, *J. Amer. Cerm. Soc.* **64** (1981) 37.
3. S. HORI, "Two-Component Oxide Ceramics from CVD Powders", (Uchida Rokakuhou, Tokyo, 1988).
4. H. YOSHIMATSU, Y. MIURA, A. OSAKA, H. KAWASAKI, and S. OHMORI, *J. Mater. Sci.* **25** (1990) 5231.
5. A. H. HEUER, N. CLAUSSEN, W. M. KRIVEN and M. RÜHLE, *J. Amer. Ceram. Soc.* **65** (1982) 642.
6. H. YOSHIMATSU, H. KAWASAKI and A. OSAKA, *J. Mater. Sci.* **23** (1988) 332.
7. H. YOSHIMATSU, T. YABUKI and H. KAWASAKI, *J. Non-Cryst. Solids.* **100** (1988) 413.
8. H. YOSHIMATSU, Y. MIURA, A. OSAKA and H. KAWASAKI, *Mater. Lett.* **8** (1989) 123.
9. *Idem., J. Mater. Sci.* **25** (1990) 961.
10. "Technical Catalogue" (Kawaken Fine Chemical Co., Ltd. Tokyo, Japan).
11. H. TORAYA, M. YOSHIMURA and S. SOMIYA, *J. Amer. Ceram. Soc.* **67** (1984) C119.
12. "Technical Letter" (Takeo Fine Chemical Co., Ltd., Takeo-shi, Japan).

Received 6 June 1994
and accepted 1 December 1995